Journal of Luminescence 196 (2018) 379–386

Contents lists available at ScienceDirect

Journal of Luminescence

journal homepage: www.elsevier.com/locate/jlumin

A water-soluble Fe^{3+} selective fluorescent turn-on chemosensor: Preparation, theoretical study and its optical vitro imaging

Lei Wang[a,*], Wenxuan Li[a], Wenjing Zhi[a], Yun Wang[a], Juan Han[b], Zhengyang Cao[a], Liang Ni[a], Haoran Li[c], Junjie Jing[a]

[a] School of Chemistry and Chemical Engineering, Jiangsu University, Zhenjiang 212013, PR China
[b] School of Food and Biological Engineering, Jiangsu University, Zhenjiang 212013, PR China
[c] Department of Chemistry, Zhejiang University, Hangzhou 310027, PR China

ARTICLE INFO

Keywords:
Chemosensor
Iron cation
Fluorescence enhancement
Cellular imaging

ABSTRACT

A rhodamine derivative bearing a thiazole receptor (probe **1**) was developed and characterized. Probe **1** rendered a prominently chromogenic and turn-on fluorescent signal toward Fe^{3+} ion in aqueous media based on coordination reaction. Probe **1** also showed high sensitivity toward Fe^{3+} ion with the detection limit as low as 92 nM. By means of the Job's plot, 2:1 binding mode of **1**-Fe^{3+} complex was determined and a possible sensing mechanism was further proposed based on the changes in the Fourier Transform Infrared (FT-IR) and mass spectra. The turn-on fluorescence and sensing mechanism for **1**-Fe^{3+} complex were well demonstrated by theoretical calculations. Importantly, probe **1** has been tested highly suitable for mapping Fe^{3+} ion in human colon cancer cells SW480, providing a wonderful candidate for tracking Fe^{3+} in biological processes.

1. Introduction

Development of ion sensors for selective recognition of heavy metal ions (HMs) is critical for a host of pertinent biological, environmental and diagnostic applications [1]. Amongst these heavy metal ions, Fe^{3+} ion is one of the most concerning metals, which plays a critical role in living system and also affects human health [2]. For example, excess or deficiency of Fe^{3+} ions can cause a series of serious diseases, such as nucleic acid and protein damage, anemia, low blood pressure and decreased immunity [3]. Recently, various probes capable of the detection of Fe^{3+} ions have been developed [4–6]. However, lack of selectivity and poor water solubility are the main limitations associated with most Fe^{3+} sensing probes [7–9]. Therefore, there is a need for developing new probes that can be applicable in aqueous solution and render good selective detection in presence of analogous ions.

Rhodamine derivatives are widely used as fluorescent probes since the pioneering work of Czarnik group [10]. As is well known, its non-fluorescent spirolactam form can be converted into its strong fluorescent ring-opened amide form by specific ions [11,12]. Based on the changes in the fluorescence, water-soluble rhodamine-based probes have been intensively studied for detecting Fe^{3+} ions [13,14]. But these probes still possess some inadequacies, such as significant interference and low sensitivity. To overcome these drawbacks, thiazole is employed as the receptor to coordinate with Fe^{3+} ion. Thiazole with the lone pair electrons at its nitrogen and sulfur atoms offers a good chance for the coordination with Fe^{3+} ion [15].

In our study, a new probe composed of rhodamine hydrazide and thiazole was designed and synthesized (Scheme 1). The probe **1** had high affinity for Fe^{3+} ion, in which the O, N and S atoms offer binding sites to the Fe^{3+} ion. The probe **1** also possessed high sensitivity with the detection limit as low as 92 nM. Upon treatment with Fe^{3+} ion, probe **1** displayed turn-on red fluorescence in aqueous media under physiological pH. Experimentally observed spectroscopic properties of **1** and its Fe^{3+} complex have been well substantiated by theoretical calculations using density functional theory. Furthermore, it can be used for fluorescence imaging of the Fe^{3+} ion in living cells.

2. Experimental section

2.1. Materials and apparatus

All the materials for synthesis and analysis were purchased from commercial suppliers and used as received. Deionized water was used throughout the entire experiments. UV–vis absorption spectra were performed using the Shimadzu UV-2450 spectrometer. The pH measurements were determined by PHS-3D digital pH-meter. Fourier Transform Infrared (FT-IR) spectroscopy were conducted upon Nicolet Nexus 470 spectrometer with KBr disks. Fluorescence spectra were

* Corresponding author.
E-mail address: wanglei86@ujs.edu.cn (L. Wang).

https://doi.org/10.1016/j.jlumin.2017.12.061
Received 4 August 2017; Received in revised form 27 November 2017; Accepted 27 December 2017
Available online 30 December 2017
0022-2313/

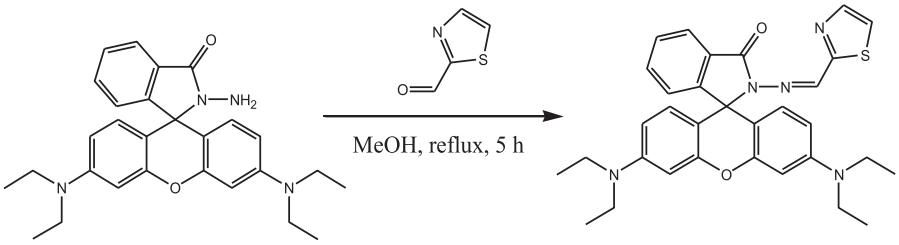

Scheme 1. Synthetic route of probe **1**.

recorded with a Cary Eclipse fluorescence spectrophotometer. The ^{1}H NMR and ^{13}C NMR spectra were collected on a Bruker AVANCEII400 MHz spectroscopy. Mass spectra were observed using a High Performance Liquid Chromatography-Mass spectrometry of MS spectrometer. Fluorescence images were taken on an inverted fluorescence microscope.

2.2. Synthesis of probe 1

The Rhodamine B hydrazide (RbH) was synthesized based on reported literature [16]. RbH (1.0 g, 2.004 mmol) was dissolved in absolute methanol (20 mL). 1,3-thiazole-2-carbaldehyde (0.565 g, 5.000 mmol) was added to the above solution and pH value was adjusted to 5 using acetic acid. After heating to reflux for 5 h with vigorously stirring, the mixture was allowed to cool and freeze below 0 °C for 8 h. The resulting precipitate was filtered and washed with methanol for three times. With the desiccation completed, the reaction afforded probe **1** as yellow solid (1.05 g, 85.64%). FT-IR (KBr, cm^{-1}, Fig. S1): 2972, 1721,1691, 1632, 1613, 1546, 1516, 1467, 1427, 1356, 1336, 1303, 1261, 1232, 1218, 1118, 789. ^{1}H NMR (400 MHz, $CDCl_3$, Fig. S2) δ 8.52 (s, 1H), 8.03 (d, J = 7.2 Hz, 1 H), 7.75 (d, J = 3.1 Hz, 1 H), 7.51 (dd, J = 11.8, 7.8 Hz, 2 H), 7.27 (dd, J = 3.2, 0.8 Hz, 1 H), 7.15 (d, J = 7.4 Hz, 1 H), 6.55 (d, J = 8.8 Hz, 2 H), 6.46 (s, 2 H), 6.26 (d, J = 7.9 Hz, 2 H), 3.34 (q, J = 6.9 Hz, 8 H), 1.17 (t, J = 7.0 Hz, 12 H). ^{13}C NMR (101 MHz, $CDCl_3$, Fig. S3) δ 166.86, 165.11, 153.00, 152.19, 149.10, 143.37, 139.56, 133.91, 128.39, 128.03, 127.62, 123.85, 123.66, 120.34, 108.06, 105.13, 98.23, 66.04, 44.32, 12.62. MS (Fig. S4): m/z calculated for $C_{32}H_{33}N_5O_2S$ 551.24 $[M]^+$, found 552.54 $[M+H]^+$.

2.3. The stock solution details

Probe **1** was prepared in ethanol to afford 1 mM stock solution. A variety of metal ions, Fe^{3+}, Li^{+}, Ni^{2+}, Hg^{2+}, Co^{2+}, Fe^{2+}, Sr^{2+}, Cu^{2+}, Pb^{2+}, Cd^{2+}, Ca^{2+}, Mg^{2+}, Zn^{2+}, $Cr^{3+}$and Al^{3+}, dissolved in deionized water was used as 10 mM stock solutions. The solutions of various testing metal ions were prepared from corresponding chloride salts.

2.4. The detection limit study

According to the study of fluorescence titrations, the detection limit (LOD) of probe **1** with Fe^{3+} was discussed. The emission intensity of probe **1** toward Fe^{3+} was determined after measuring twenty times and the standard curve was plotted. The detection limit was then calculated on the basis of LOD = 3σ/k, where k characterizes to the slope of the standard curve, with σ characterizes the standard deviation of blank measurement [17].

2.5. Computational study of probe 1

Calculations on **1** and **1**-Fe^{3+} complex were performed with density functional theory (DFT) using the Gaussian 09 program. The 6–311G** basis sets was employed for main group elements, whereas the LanL2DZ basis sets was applied for Fe^{3+}. On account of energy-minimized structures, the optimized structures of **1** and **1**-Fe^{3+} complex were acquired.

2.6. Cell incubation and biological imaging

SW480, human colon cancer cells were cultivated at a 24-well plate at 37 °C in Dulbecco's Modified Eagle's medium (DMEM) replenished with 10% fetal bovine serum (FBS) for 24 h. Subsequently, the human colon cancer cells SW480 were preprocessed with 5 μM probe **1** for 30 min, and washed the cells with HEPES buffer solution (1.0 mM, pH 7.0) for three times then imaged. In control group, the probe **1**-burdened cells were placed to 10 μM Fe^{3+} for 10 min and coincubated for 30 min. The cells were washed three times using HEPES buffer solution (1.0 mM, pH 7.0) to remove the residue of Fe^{3+} and then imaged. After that, the cellular imagings were carried out under an inverted fluorescence microscope.

3. Results and discussion

The selectivity, sensitivity and binding mode of probe **1** toward Fe^{3+} ion were characterized through fluorescence emission, naked-eye inspection, absorption band, FT-IR spectra, mass measurements and DFT calculations.

3.1. UV–vis and Fluorescence spectral studies of probe 1 in the presence of metal ions

The chemosensing behavior of probe **1** with various metal ions in HEPES buffer solution (1.0 mM, pH 7.0) was evaluated by UV–vis absorption spectrometry. As displayed in Fig. 1, only addition of 200 μM of Fe^{3+} ion, the probe **1** (10 μM) displayed a dramatic change in the UV–vis spectra with a new absorption band appearing at 567 nm for **1**-Fe^{3+} complex. Concomitantly, a prominent purple color developed that allowed colorimetric detection of Fe^{3+} ion, as shown in the illustration of Fig. 1. Whereas, no significant sensing response of probe **1** (10 μM) occurred in the presence of 200 μM of other metal ions such as Li^{+}, Ni^{2+}, Hg^{2+}, Co^{2+}, Fe^{2+}, Sr^{2+}, Cu^{2+}, Pb^{2+}, Cd^{2+}, Ca^{2+}, Mg^{2+}, Zn^{2+}, Cr^{3+} and Al^{3+}, except for Cr^{3+} and Al^{3+} ions which exhibited a weak response (Fig. S5). These results validated the selectivity of probe **1** toward Fe^{3+} ion.

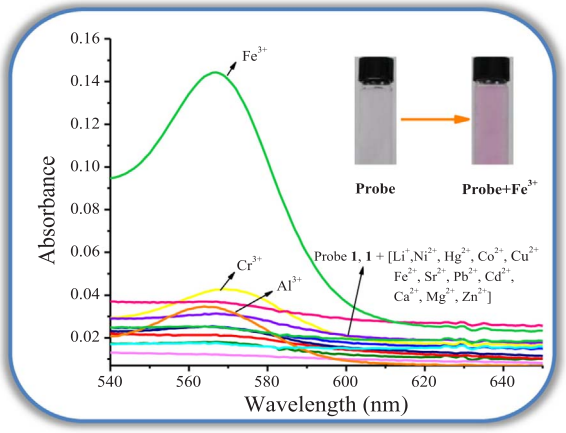

Fig. 1. Absorption spectra of probe **1** (10 μM) in the presence of 200 μM of various metal ions in HEPES buffer solution (1.0 mM, pH 7.0).